Virus Inhibition Activity of Effector Memory CD8+ T Cells Determines Simian Immunodeficiency Virus Load in Vaccinated Monkeys after Vaccine Breakthrough Infection

Takuya Yamamoto,[a] Matthew J. Johnson,[a] David A. Price,[a,b] David I. Wolinsky,[a] Jorge R. Almeida,[a] Constantinos Petrovas,[a] Martha Nason,[c] Wendy W. Yeh,[d] Ling Shen,[d] Mario Roederer,[a] Srinivas S. Rao,[a] Adrian B. McDermott,[a] Francois Lefebvre,[e] Gary J. Nabel,[a] Elias K. Haddad,[e] Norman L. Letvin,[d] Daniel C. Douek,[a] and Richard A. Koup[a]

Vaccine Research Center[a] and Biostatistics Research Branch,[c] NIAID, NIH, Bethesda, Maryland, USA; Department of Infection, Immunity and Biochemistry, Cardiff University School of Medicine, Cardiff, Wales, United Kingdom[b]; Beth Israel Deaconess Medical Center, Harvard Medical School, Boston, Massachusetts, USA[d]; and VGTI-FL, Port St. Lucie, Florida, USA[e]

The goal of an effective AIDS vaccine is to generate immunity that will prevent human immunodeficiency virus 1 (HIV-1) acquisition. Despite limited progress toward this goal, renewed optimism has followed the recent success of the RV144 vaccine trial in Thailand. However, the lack of complete protection in this trial suggests that breakthroughs, where infection occurs despite adequate vaccination, will be a reality for many vaccine candidates. We previously reported that neutralizing antibodies elicited by DNA prime-recombinant adenovirus serotype 5 (rAd5) boost vaccination with simian immunodeficiency virus strain mac239 (SIVmac239) Gag-Pol and Env provided protection against pathogenic SIVsmE660 acquisition after repeated mucosal challenge. Here, we report that SIV-specific CD8+ T cells elicited by that vaccine lowered both peak and set-point viral loads in macaques that became infected despite vaccination. These SIV-specific CD8+ T cells showed strong virus-inhibitory activity (VIA) and displayed an effector memory (EM) phenotype. VIA correlated with high levels of CD107a mobilization and perforin expression in SIV-specific CD8+ T cells. Remarkably, both the frequency and the number of Gag CM9-specific public clonotypes were strongly correlated with VIA mediated by EM CD8+ T cells. The ability to elicit such virus-specific EM CD8+ T cells might contribute substantially to an efficacious HIV/AIDS vaccine, even after breakthrough infection.

Multiple lines of evidence indicate that virus-specific CD8+ T cells are responsible for the immediate and long-term control of human immunodeficiency virus (HIV) and simian immunodeficiency virus (SIV) replication *in vivo* (5, 10, 17, 28). Thus, the ability to elicit a durable and potent HIV-1-specific CD8+ T cell response following vaccination will remain an important characteristic of vaccines that do not achieve full sterilizing immunity in all vaccinees. The measurement of virus inhibition *ex vivo* and *in vitro*, using infected primary autologous CD4+ T cells as targets, encompasses the totality of the potential inhibitory mechanisms deployed by CD8+ T cells (7). Therefore, the virus inhibition assay measures the overall potency of the CD8+ T cell-mediated antiviral response elicited by infection or vaccination.

A public clonotype specific for a particular epitope is defined as a T cell receptor beta (TCRB) amino acid sequence that occurs in more than one individual (32). Previous work has shown that CM9-specific public clonotype usage predicts the set-point viral load (VL) that emerges during early-chronic-phase infection (22, 32). Despite significant work to clarify the mechanism underlying the generation of public clonotypes and the viral control offered by them (2, 6, 21, 23, 30, 31), our understanding of how they mediate protection is far from complete. Thus, a comprehensive understanding of the TCR traits that can predict immune responses and viral outcomes is warranted in future efficacious vaccine trials.

We have shown previously that immunization with a DNA prime-recombinant adenovirus serotype 5 (rAd5) boost vaccine comprising SIVmac239 Gag-Pol and Env protected Mamu-A*01+ rhesus macaques against SIVsmE660 infection (19). The protection was incomplete but correlated with the induction of

SIV-specific neutralizing antibodies. In addition, macaques expressing two TRIM5 alleles that restrict SIV replication were more likely to be protected from infection than macaques expressing at least one permissive TRIM5 allele. Here, we determined whether this vaccine also had an impact on virologic control in those macaques that became infected despite vaccination. Our results show that vaccine-induced SIV-specific effector memory (EM) CD8+ T cells that display strong virus-inhibitory activity (VIA) and incorporate public TCRs are associated with SIV control in macaques with breakthrough infection.

MATERIALS AND METHODS

Animals. Adult rhesus monkeys of Indian origin were used in the study after full protocol approvals from the Institutional Animal Care and Use Committees of the Vaccine Research Center, NIAID, NIH, and Bioqual, Inc., where the animals were housed. Both institutions are fully accredited by the Association for Accreditation of Laboratory Animal Care, International (AAALAC,I). All experiments were conducted in accordance with the Guide for the Care and Use of Laboratory Animals (20) and all institutional, state, and federal guidelines.

Rhesus monkeys were immunized with plasmid DNA (4 mg per construct, intramuscularly, at weeks 0, 4, and 8) and rAd5 vectors (1×10^{11}

particles per construct, intramuscularly, at week 26) using vectors expressing SIVmac239 Gag-Pol and Env.

Viral load quantification. Plasma SIV RNA was determined for all SIVsmE660 studies using previously published protocols (19).

Antibodies. The following directly conjugated monoclonal antibodies (MAbs) were used: CD3-Cy7APC, CD107a-FITC, IL-2-Cy5.5PerCP, MIP-1β-PE, IFN-γ-V450, and CD95-Cy7PE (BD Biosciences), CD28-TexasRedPE (Beckman Coulter), granzyme-B-Cy5.5PE, CD4-Qdot605, and CD8-Qdot655 (Invitrogen), PD-1-Cy5.5PerCP and granzyme-A-pacific blue (Biolegend), and perforin-FITC (Mabtech). Aqua amine reactive viability dyes were obtained from Invitrogen.

Polychromatic flow cytometry. Cells were analyzed using a modified LSR II flow cytometer (BD Immunocytometry Systems) as described previously (18). Briefly, 2×10^6 peripheral blood mononuclear cells (PBMCs) were incubated in 1 ml of RPMI 1640 medium supplemented with 10% fetal bovine serum (FBS) and penicillin/streptomycin that contained monensin (0.7 μg/ml; BD Biosciences) and brefeldin A (10 μg/ml; Sigma-Aldrich) in the absence or presence of CD107a MAbs and peptides (15mers overlapping by 11 residues) corresponding to full-length SIVmac239 Gag (2 μg/ml for each peptide at 5 μl/ml; National Institutes of Health AIDS Research and Reference Reagent Program) for 6 h. After washing, cells were surface stained for CD4, CD8, CD28, and CD95; aqua amine reactive dye was used to exclude dead cells from the analysis. Following permeabilization (Cytofix/Cytoperm kit; BD Biosciences), cells were stained for CD3, gamma interferon (IFN-γ), interleukin 2 (IL-2), MIP-1β, and tumor necrosis factor alpha (TNF-α). Between 3×10^5 and 1×10^6 events were collected in each case. Electronic compensation was conducted with MAb capture beads (BD Biosciences) stained separately with the individual MAbs used in the test samples. Data were analyzed using FlowJo version 9.3.3 (TreeStar). Forward scatter area versus forward scatter height was used to gate out cell aggregates. CD14^{+}, CD19^{+}, and dead cells were removed from the analysis to reduce background staining.

Peptide-major histocompatibility complex (MHC) class I tetramers. Soluble fluorochrome-labeled peptide-Mamu-A*01 (pMamu-A*01) SIV Gag CM9-specific tetramers were produced and used as described previously (22, 23) (CM9; CTPYDINQM, residues 181 to 189). For phenotypic analyses of pMamu-A*01–allophycocyanin (APC) tetramer-labeled cells, between 3×10^5 and 1×10^6 events were acquired on an LSR II flow cytometer (BD). The following reagents and MAb specificities were used: aqua, CD3, CD4, CD8, CD28, CD95, PD-1, perforin, granzyme A, and granzyme B.

Virus inhibition assay. Virus-inhibitory activity (VIA) was measured as follows. PBMCs from each macaque were thawed in RPMI 1640 supplemented with 10% FBS and penicillin/streptomycin and stimulated with concanavalin A (25 μg/ml) in the presence of recombinant human interleukin-2 (rhIL-2) at a concentration of 50 U/ml (PeproTech). After stimulation for 1 day, the medium was replenished and the cells were incubated for an additional day. PBMC targets were depleted of CD8^{+} cells using a magnetically activated cell sorting (MACS) nonhuman primate CD8 MicroBead kit (Miltenyi Biotec) according to the manufacturer's instructions. Effector memory (EM) CD8^{+} T cells were sorted by flow cytometry using the fluorescence-activated cell sorter (FACS) Aria (BD) based on the differential expression of CD28 and CD95. Target PBMCs were infected at 1×10^6 cells/ml using a multiplicity of infection (MOI) of 0.004 to 0.06 by spinoculation at $1,200 \times g$ for 2 h. Following spinoculation, cells were resuspended and plated at 4×10^4 cells per well in a flat-bottom 96-well tissue culture plate. EM CD8^{+} T cells were serially diluted 2-fold from 2×10^5 to 4×10^4 cells/ml and added to autologous infected targets at corresponding effector/target (E:T) ratios of 5:1, 2:1, and 1:1. Infectivity controls consisted of infected targets without added CD8^{+} effectors. Cultures were incubated at 37°C and 5% CO$_2$ for 3 or 5 days. Viral replication was measured by the SIV p27 antigen capture assay (Advanced BioScience Laboratories Inc.). Viral inhibition was calculated as a percentage of the infectivity control for each E:T ratio and a log

reduction of SIV p27 levels compared to that of infectivity controls at an E:T ratio of 5:1.

Clonotype analysis. Viable tetramer-stained central memory (CM), EM, and total CD8^{+} T cells were sorted by flow cytometry at >98% purity into 1.5-ml microtubes containing 150 μl RNAlater. The number of sorted cells for each CM9-specific population ranged from 470 to 5,000 cells. mRNA was extracted using the μMACS mRNA isolation kit (Miltenyi Biotec). Unbiased amplification of all expressed *TRB* gene products was achieved using a template switch-anchored reverse transcriptase (RT)-PCR (25). Amplicons were subcloned and sequenced as described previously (6, 25). Sequence reads were analyzed to determine T cell receptor beta variable (TRBV) and T cell receptor beta joining (TRBJ) gene usage, CDR3 sequences, and CDR3 length.

Microarray and pathway analysis. Gag CM9-specific EM CD8^{+} T cells (CD28^{low}CD95^{high} tetramer^{+}) from SIV-negative macaques at 12 weeks post-DNA/rAd5 immunization were sorted by flow cytometry as described above for microarray studies. Eleven RNA samples from two groups based on the VIA data (CM9 peptide-stimulated cells from macaques with strong VIA or those with weak VIA) and two groups based on cell treatment (cells from macaques with strong VIA with or without CM9 peptide stimulation) were prepared using the Illumina beads station assay as described previously (8, 24) and hybridized to the Illumina HumanHT-12 version 4 Expression BeadChip according to the manufacturer's instructions. Analysis of the GenomeStudio output data was conducted using the R statistical language (27) and various software packages from Bioconductor (9). Quantile normalization was applied, followed by a log$_2$ transformation. The LIMMA package (29) was used to fit a single linear model to each probe and to perform (moderated) t tests on the differences of interest. Two differences were tested, the first between CM9 peptide-stimulated and nonstimulated CM9^{+} EM CD8^{+} T cells from macaques with strong VIA and the second between CM9 peptide-stimulated CM9^{+} EM CD8^{+} T cells from monkeys with strong VIA and those from monkeys with weak VIA. The expected proportions of false positives (false discovery rate [FDR]) were estimated from the unadjusted P values using the Benjamini and Hochberg method. Pathway, functional, and network analysis were conducted with ingenuity pathway analysis (IPA; Ingenuity Systems, Redwood City, CA). The input data include genes whose expression levels met the following criteria: fold change of ≥1.5 (up or down) and raw P value of <0.01. The genes in the data were mapped to the ingenuity pathway knowledge base with different colors (red, upregulated; green, downregulated), and the networks for immunological disease, inflammatory disease, and neurological disease were further explored.

TRIM5 genotyping. Genomic DNA was isolated from lymphocytes using the QIAamp DNA kit (Qiagen) and sequenced for *TRIM5* exons as described previously (19).

Statistical analysis. Experimental variables were analyzed using the nonparametric Mann-Whitney U test and the Wilcoxon matched-pairs signed-rank test. Correlations were performed using the nonparametric Spearman rank test. Bars depict median values; P values of <0.05 were considered significant. The GraphPad Prism statistical analysis program (GraphPad Software) was used throughout. Analysis and graphical representation of cytokine production were conducted using the data analysis program Simplified Presentation of Incredibly Complex Evaluations (SPICE; version 5.2), provided by M. Roederer, National Institutes of Health, Bethesda, MD.

Microarray data accession number. All data were deposited in a public repository, the National Center for Biotechnology Information Gene Expression Omnibus (GEO), and can be accessed at http://www.ncbi.nlm.nih.gov/geo (accession no. GSE35628).

RESULTS

The DNA prime-rAd5 boost elicits CD8 T cell-mediated virus inhibition. Thirty-nine Mamu-A*01 rhesus monkeys were given
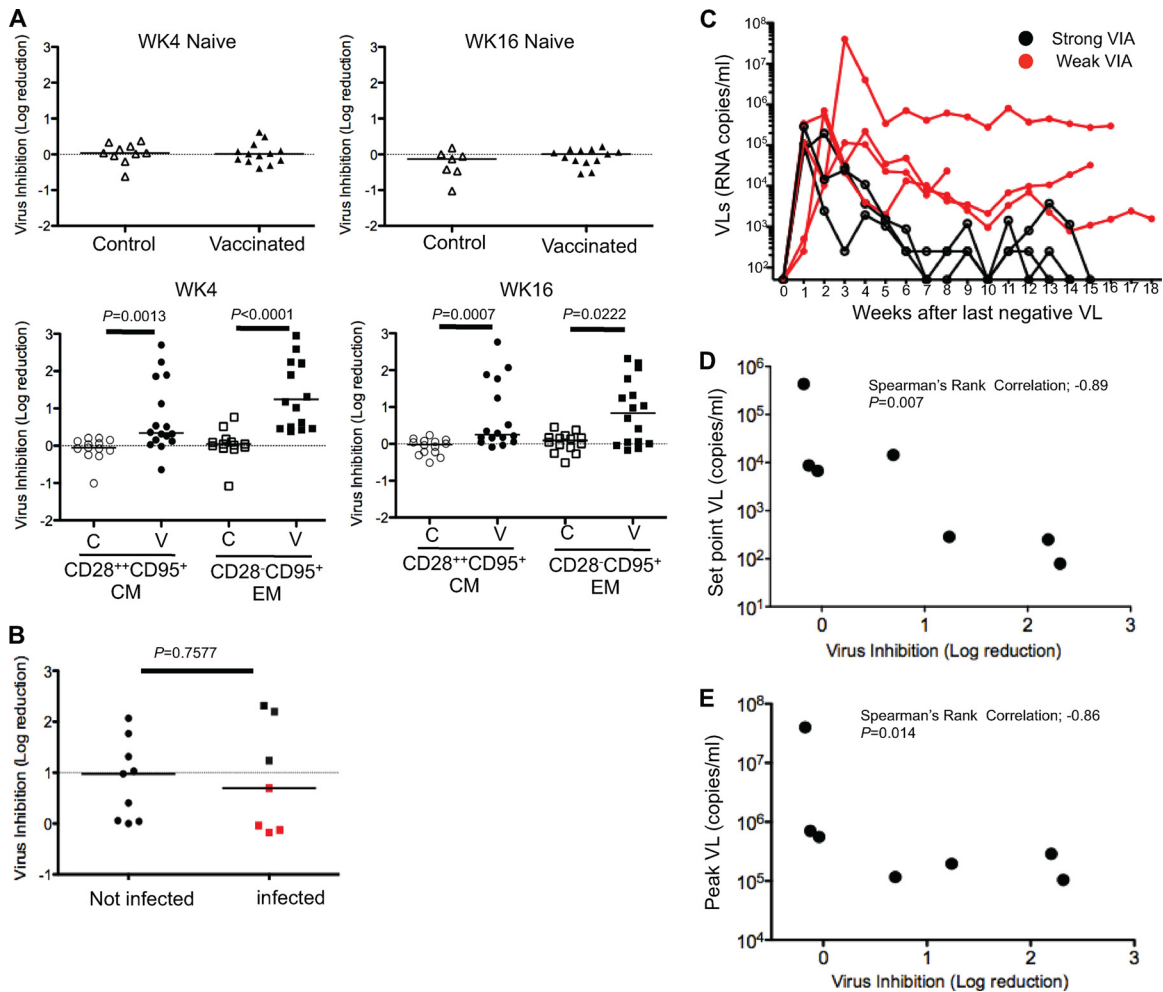
FIG 1 Relationship between VIA and control of SIV replication. (A) The upper panels show the VIA of naïve CD8^{+} T cells against SIVsmE660 for 10 control macaques and 13 vaccinated macaques at week 4 (WK4) after the rAd5 boost and for 7 control macaques and 13 vaccinated macaques at week 16 (WK16) after the rAd5 boost. The lower panels show pooled data for the log reduction of SIV replication at week 4 after the rAd5 boost (CM, $n = 13$; EM, $n = 16$) and at week 16 after the rAd5 boost (CM, $n = 14$; EM, $n = 16$). The inhibition is calculated as the $\log_{10}$ reduction in virus infection, measured by an SIV Gag p27 enzyme-linked immunosorbent assay (ELISA), compared to that of the autologous infectivity controls. The dotted line shows no reduction. P values were calculated using the Mann-Whitney U test. (B) Pooled data of VIA against SIVsmE660 in vaccinated macaques, comparing infection outcomes after repeated mucosal challenge. A threshold for positive antiviral activity was established at 3 standard deviations above a 1-log reduction. Red dots represent infected macaques that exhibited less than 1 log of VIA. (C) Longitudinal VL measurements are shown for each macaque over an 18-week period from time of infection. Red lines represent macaques that displayed less than 1 log of VIA (weak VIA). Black lines represent the macaques that displayed more than 1 log of VIA (strong VIA). (D) Simple linear regressions predicting mean set-point $\log_{10}$ VLs from weeks 6 to 9 after infection by VIA within the EM CD8^{+} T cell population at week 16 after the rAd5 boost ($n = 7$). (E) Simple linear regressions predicting mean peak $\log_{10}$ VLs by VIA within the EM CD8^{+} T cell population at week 16 after the rAd5 boost ($n = 7$).

the DNA prime-rAd5 boost vaccine encoding either SIVmac239 Gag-Pol and Env or a placebo and were subsequently challenged by repeated rectal inoculation with SIVsmE660. While protection was afforded by the vaccine, seven vaccinated monkeys became infected (19) (see Fig. S1A in the supplemental material).

No VIA was detected in naïve CD8^{+} T cells at week 4 and week 16 post-rAd5 boost in either control or vaccinated monkeys (Fig. 1A, upper). However, at week 4 postboost, VIA was detected in both central memory (CM) and effector memory (EM) CD8^{+} T cells within the vaccinated monkeys (Fig. 1A, lower) (CM, $P = 0.0013$; EM, $P < 0.0001$). VIA persisted through week 16 postboost (CM, $P = 0.0007$; EM, $P = 0.0222$) and was not related to the number of *TRIM5* alleles that restrict SIV replication (see Fig. S1B in the supplemental material).

We compared VIAs in vaccinated macaques by whether or not they became infected after repeated rectal challenge with SIVsmE660. No differences in VIA were apparent between the two groups (Fig. 1B) ($P = 0.7577$). These data agree with a prior report which showed no association between either CD8^{+} T cells or innate immune responses and protection against virus acquisition (19). However, among the macaques that became infected, those with more than 1 log of vaccine-induced VIA (strong VIA) within the EM CD8^{+} T cell compartment showed lower plasma VLs than those with less than 1 log of VIA (weak VIA) (Fig. 1C). We did not observe any relationship between VIA within CM CD8^{+} T cells and VL at any time point (see Fig. S1C in the supplemental material).

There was an inverse correlation between set-point VL and prechallenge VIA within EM CD8^{+} T cells (Fig. 1D) ($P = 0.007$,
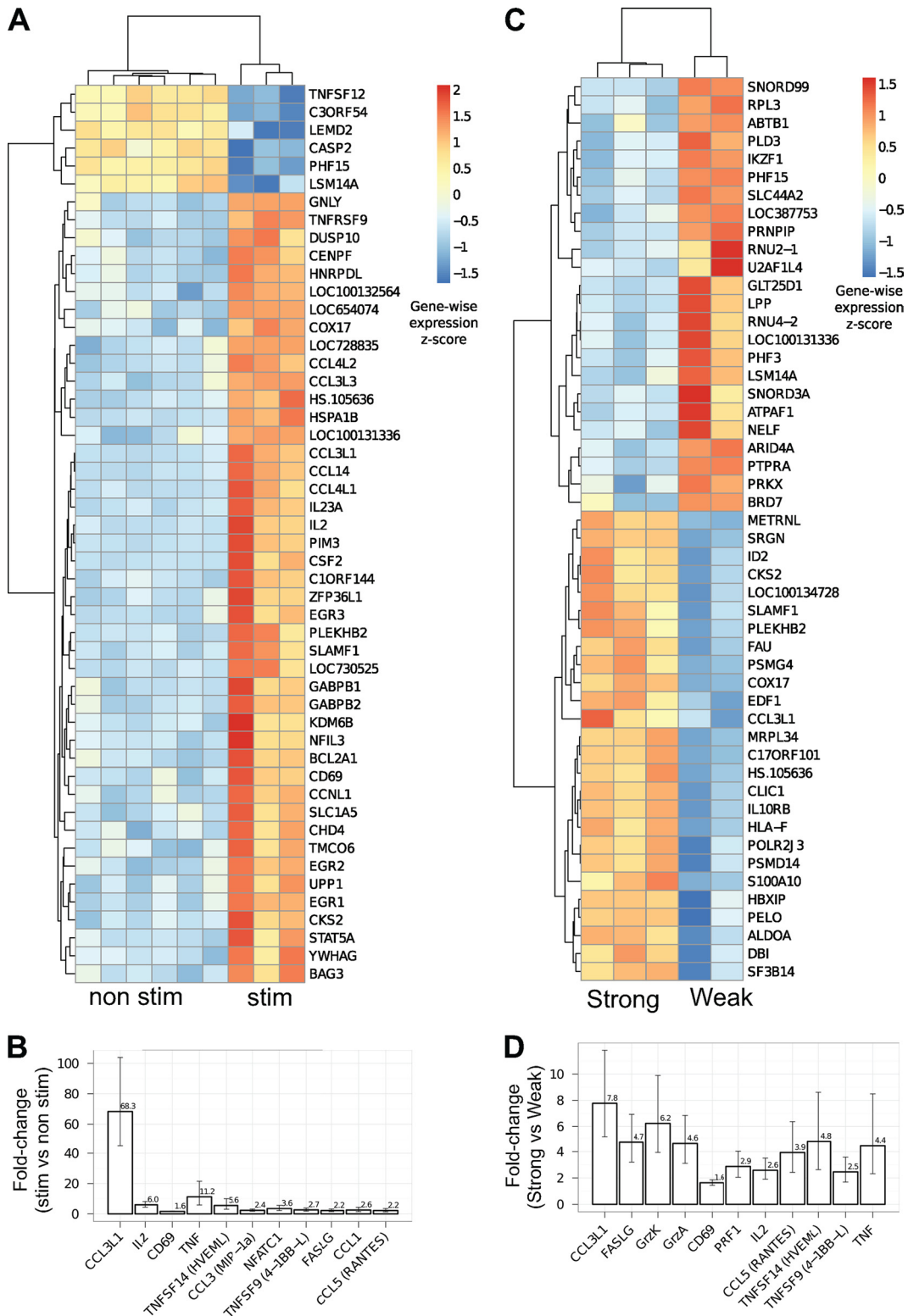
FIG 2 CM9-specific EM CD8$^+$ T cells with strong VIA exhibit a transcriptional profile distinct from that of cells with weak VIA. (A) Heat map representation of the expression values for the top 50 (FDR estimated at 0.09%) genes that are most significantly differentially expressed between nonstimulated CM9-specific EM CD8$^+$ T cells ($n = 6$) and stimulated CM9-specific EM CD8$^+$ T cells ($n = 3$). Rows represent genes, and columns represent samples. Colors correspond to the value of the within-gene (row) standard score. (B) Relative (stim versus nonstim) expression levels of stimulated CM9-specific EM CD8$^+$ T cells for a selection of 11 functionally relevant genes. All genes meet the requirement of a P value of <0.005 and are found at a 5% FDR except for FASLG (9%), CCL1 (17%), and CCL5 (22%). Panels C and D are the same as panels A and B except that they show the comparison between stimulated CM9-specific EM CD8$^+$ T cells with strong VIA ($n = 2$) and stimulated CM9-specific EM CD8$^+$ T cells with weak VIA ($n = 3$). The FDR in panel C is estimated at 0.3%. Selected genes in panel D meet the requirement of a P value of <0.003 and are found at 5% FDR except for TNFSF14 (7%), TNFSF9 (10%), and TNF (12%).
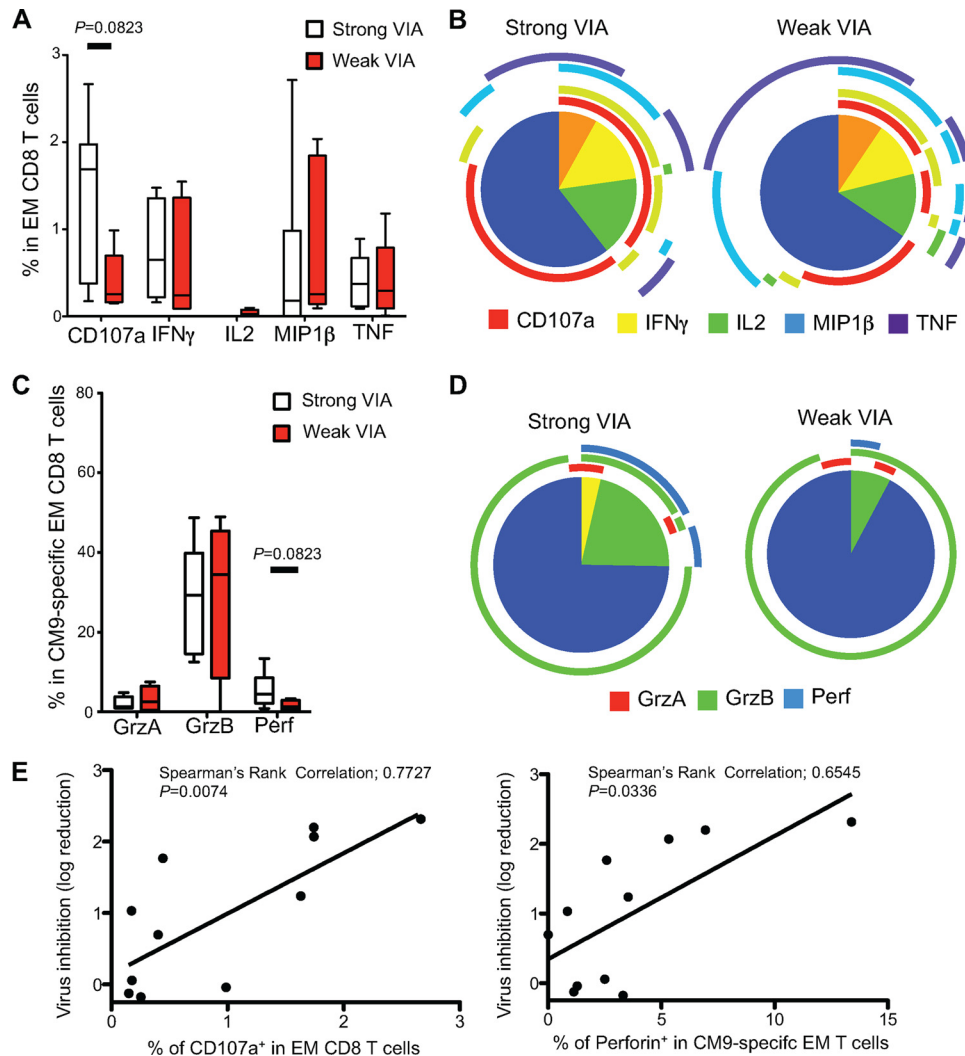
FIG 3 Functional profiles of SIV-specific CD8$^+$ T cell responses. (A to D) Flow cytometric analysis of CD107a mobilization and the production of IFN-γ, IL-2, MIP-1β, TNF, granzyme A, granzyme B, and perforin within Gag-specific CD8$^+$ T cells. (A and C) The proportions of the total Gag-specific CD8$^+$ T cell response contributed by each function in macaques with strong VIA ($n = 6$; open) and weak VIA ($n = 5$; red) are shown, with boxes representing interquartile ranges. The magnitude of the Gag-specific response in total EM CD8$^+$ T cells (A) or the CM9-specific response in CM9-specific EM CD8$^+$ T cells (C) was calculated based on the summation of all individual functional response patterns. Horizontal bars represent median values. (B) The pie charts show the fractions of cells with 1, 2, 3, 4, and 5 functions. The color-coded circles indicate the proportions of the 5, 4, 3, 2, and 1 functional responses that are contributed by the single cytokines CD107a (red), IFN-γ, (yellow), IL-2 (green), MIP-1β (blue), and TNF (purple). (D) The pie charts show the fractions of cells with 1, 2, and 3 functions. The color-coded circles indicate the proportions of the 3, 2, and 1 functional responses that are contributed by the single cytolytic enzymes granzyme A (red), granzyme B (green), and perforin (blue). (E) Simple linear regressions predicting the percentage of CD107a$^+$ Gag-specific EM CD8$^+$ T cells (left) and the percentage of perforin-positive (perforin$^+$) CM9-specific EM CD8$^+$ T cells (right) by VIA within the EM CD8$^+$ T cell population at week 16 after the rAd5 boost ($n = 11$).

$r = -0.89$). This inverse correlation was also observed between peak VL and prechallenge VIA within EM CD8$^+$ T cells (Fig. 1E). Neither the peak nor set-point VL was related to the frequency of CM9-specific CD8$^+$ T cells in either the EM or total CD8$^+$ T cells (see Fig. S2A to D in the supplemental material). In addition, there was no relationship between the VIA of EM CD8$^+$ T cells and the frequency of CM9-specific CD8$^+$ T cells in either the EM or total CD8$^+$ T cell compartments (see Fig. S2E and F in the supplemental material).

Molecular gene signature of Gag CM9-specific EM CD8$^+$ T cells. Microarray gene analysis was performed on immunodominant CM9-specific EM CD8$^+$ T cells. CM9-specific EM CD8$^+$ T cells from macaques with strong VIA were sorted by flow cytometry with (stim) or without (nonstim) prior CM9 peptide stimulation. (stim, $n = 3$; nonstim, $n = 6$). A heat map representation of the 50 genes most significantly upregulated after CM9 stimulation is shown in Fig. 2A, while Table S1 in the supplemental material provides the full list of 677 upregulated genes. A selection of genes known to be upregulated with TCR stimulation and related to the functional activities of CD8$^+$ T cells is shown in Fig. 2B. We observed significant increases in the expression of genes encoding cytokines (TNF, IL-2), chemokines (CCL1, CCL3, CCL5, and CCL3L1), transcription/activation markers (CD69, NFATC1), and cytolytic molecules that are related to the killing activity of

A

ID	TRBV	CDR3 AA	TRBJ	Freq
AR96	2.3	CASTSRDSASQNTQY	2.4	26.3
	6.3	CASSYGGNSNQPQY	1.5	25.0
	6.2	CASSEALHQTDPQY	2.3	12.5
	10.2	CASSGQGNSNQPQY	1.5	8.8
	6.2	CASSEALRGADPQY	2.3	6.3
	6.2	CASSEGGNSNQPQY	1.5	6.3
	23	CASSQGHLSNQPQY	1.5	5.0
	6.1	CASSLQGNSNQPQY	1.5	3.8
	6.2	CASSLQGNSNQPQY	1.5	1.3
	10.2	CASRPGQGKDPQY	2.3	2.5
	11.1	CASSSLGKSYEQY	2.7	1.3
	6.1	CASSEARRGADPQY	2.3	1.3
ZD51	6.1	CASSNNGNSNQPQY	1.5	17.9
	6.1	CASSEANRADNEQF	2.1	11.5
	6.3	CASSEQGNTNSPLY	1.6A	10.3
	7.10	CASSPGIGYEQY	2.7	9.0
	27	CASSFDRPPDPQY	2.3	7.7
	12.2	CASSPDTHSNQPQY	1.5	5.1
	6.1	CASSEARRTSDPQY	2.3	3.8
	2.1	CASRAGGGEVSQY	2.4	3.8
	21	CASSNAEFYNSPLY	1.6A	3.8
	5.8	CTSSSKRLRDRKSYEQY	2.7	2.6
	28	CASSLSQGAISGASVLT	2.6	2.6
	7.4	CASSLYEYVDTQY	2.4	2.6
	20	CSAKESSYEQY	2.7	2.6
	7.4	CASSLRDRSNEKLF	1.4	2.6
	7.3	CASSLSGGAQTHRAF	1.1	1.3
	12.2	CASSFNQGRYDYT	1.2	1.3
	2.3	CASSGGGQGLTNEKLF	1.4	1.3
	23	CASSQSDRGAHSNQPQY	1.5	1.3
	23	CASSQSLGTGQNTQY	2.4	1.3
	9	CASSRNTGTQRGNEQF	2.1	1.3
	28	CASSSTGKHYDYT	1.2	1.3
	6.3	CASSYAGNSNQPQY	1.5	1.3
	6.3	CASSYQGNSNQPQY	1.5	1.3
	6.3	CASSYSYRAADPQY	2.3	1.3
ZD12	7.4	CASSLDPRSYNSPLY	1.6A	19.0
	6.2	CASSEALRADDPQY	2.3	17.7
	6.2	CASSEAHRANEQF	2.1	15.2
	14	CASSQGRQGREKLF	1.4	8.9
	6.1	CASSEALQGGNEQF	2.1	8.9
	6.3	CASSRTANSNQPQY	1.5	6.3
	6.2	CASSEALRGEDPQY	2.3	5.1
	6.3	CASSKQGNSNQPQY	1.5	5.1
	9	CAIVRGDEQY	2.7	3.8
	6.2	CASSEGLRGGDPQY	2.3	3.8
	14	CTSSQGRQGREKLF	1.4	1.3
	19	CASSITDRSANTAQLF	2.2	1.3
	6.1	CASSESRRADNEQF	2.1	1.3
	6.2	CASSEALRAGDPQY	2.3	1.3
	6.2	CASSEALRGGDPQY	2.3	1.3
AR44	6.1	CASSEAGNSNQPQYF	1.5	32.4
	6.3	CASSRQGNSNQPQYF	1.5	28.8
	7.4	CASSLNGNSNQPQYF	1.5	13.2
	2.2	CASSEATGTAAHTVYF	1.3	12.0
	12.2	CASSLLGGSQDTQYF	2.4	2.4
	11.1	CASSSQRDSNQPQYF	1.5	1.2
	12.2	CASSLLGGGQDTQYF	2.4	1.2
	19	CASRQLGSGNTVYF	1.3	1.2
	3.4	CASSQRGLGGVQETQYF	2.5	1.2
	6.1	CASSEARQGKNTQYF	2.4	1.2
	6.1	CASSEARTGSQPQYF	1.5	1.2
	6.1	CASSETLNSNQPQYF	1.5	1.2
	6.3	CASSRQGSSNQPQYF	1.5	1.2
	6.3	CTSSRQGNSNQPQYF	1.5	1.2
AR56	10.2	CASSESGNSNQPQYF	1.5	40.8
	10.2	CASTSGAGASVLTF	2.6	25.2
	6.3	CASSPTGRSYDYTF	1.2	21.6
	10.2	CASNQQGNSNQPQYF	1.5	14.4

B

ID	TRBV	CDR3 AA	TRBJ	Freq
AR34	13	CASSYGGYSNQPQYF	1.5	42.0
	6.1	CASTLDRVNAQLFF	2.2	22.4
	2.1	CASSEAGPPTDPQYF	2.3	5.6
	13	CASSYGGYSDQPQYF	1.5	2.8
	3.2	CASSQGGRQNEKLFF	1.4	2.8
	6.3	CASSRTGNSNQPQYF	1.5	2.8
	6.3	CASSRTRATNEKLFF	1.4	2.8
	6.3	CASSYGLGGAIRNEQFF	2.1	2.8
	10.1	CASSGDTKFYEQYF	2.7	1.4
	10.2	CASIPGQGRSPLYF	1.6A	1.4
	13	CASSFSPFGVSNQNTQYF	2.4	1.4
	13	CASSHGGYSNQPQHF	1.5	1.4
	13	CASSYGGYSNRPQYF	1.5	1.4
	2.2	CASSEFGTGGSSDPQYF	2.3	1.4
	6.1	CASIPTDRVAGASVLTF	2.6	1.4
	6.1	CASTPDRVNAQLFF	2.2	1.4
	6.1	CVSTLDRVNAQLFF	2.2	1.4
	6.3	CASSNPATIRNTQYF	2.4	1.4
	6.3	CASSRTRPTNEKLFF	1.4	1.4
AR03	13	CASNPSAYSNQPQY	1.5	38.5
	2.1	CASRGYTRNEQF	2.1	26.4
	27	CASSLSIRTGREGEAF	1.1	8.8
	11.1	CASRPGQGRQPQY	1.5	7.7
	6.3	CASSSPGTGVQNTQY	2.4	4.3
	6.1	CASSEGLRGTDPQY	2.3	3.3
	2.1	CASRGYTRNGQF	2.1	2.2
	10.2	CASSETGNSNQPQY	1.5	2.2
	5.9/5.8	CASSHSHRPYDYT	1.2	2.2
	13	CVSNPSAYSNQPQY	1.5	1.1
	27	CASSLSIRTGRGGEAF	1.1	1.1
	13	CAGNPSAYSNQPQY	1.5	1.1
	6.3	CASSYSKRGRDEQF	2.1	1.1
	6.3	CASTKMGNSNQPQY	1.5	1.1
AR76	24	CAAQRNTEAFF	1-1	60.2
	23	CASSQGTDSNQPQYF	1.5	7.0
	27	CASSLTHRVSNQPQYF	1.5	7.0
	23	CASSLKPGQVRAGNQPQYF	1.5	5.6
	7.8	CASSLATGGADPQYF	2.3	4.2
	19	CASSIARRSTDPQYF	2.3	2.8
	6.2	CASSEARRSDSPLYF	1.6A	2.8
	6.2	CASSPTGNSNQPQYF	1.5	2.8
	24	CAAQRNTETFF	1.1	1.4
	24	CAARWNTEAFF	1.1	1.4
	6.2	CASSEANRSEDPQYF	2.3	1.4
	6.3	CASSYGRTGNSPLYF	1.6A	1.4
4521	6.2	CASFLGIGTAQLF	2.2	81.9
	27	CASMSRAGGLGNTVY	1.3	3.6
	6.3	CASSYGTGYSPLY	1.6A	2.4
	23	CASSVGEYSNQPQY	1.5	2.4
	6.1	CASSATDRTFSQNTQY	2.4	2.4
	9	CASSFGTASLEQF	2.1	2.4
	6.2	CTSFLGIGTAQLF	2.2	1.2
	10.2	CASSSPETIRNTQY	2.4	1.2
	2.3	CASSEVNVSWQLREQY	2.7	1.2
	6.2	CASFLGIGTAQLL	2.2	1.2
A532	11.1	CASSLEGDRNSPLYF	1.6A	42.9
	28	CASSSRRSQFQSTQYF	2.4	28.6
	11.1	CASSLEADRNSPLYF	1.6A	6.6
	15	CASSNDLNPAQLFF	2.2	5.5
	10.2	CASSESGNSNQPQYF	1.5	3.3
	11.1	CASSLGSDRAQPQYF	1.5	3.3
	11.1	CAGSLEGDRNSPLYF	1.6A	1.1
	3.1	CASSQETALRGDPQYF	2.3	1.1
	6.1	CASSEALRAGDTEAFF	1.1	1.1
	6.1	CASSEALRQADEQFF	2.1	1.1
	6.1	CASSEVLRAGDTEAFF	1.1	1.1
	7.1	CASSKKGGVGGNTVYF	1.3	1.1
AR81	7.6	CASSSQDSSNQPQY	1.5	21.4
	3.4	CASSQGFLRTAQLF	2.2	16.7
	7.4	CASSLDRANTAQLF	2.2	10.7
	23	CASSLGQLSNQPQY	1.5	6.0
	6.1	CASSVSRVAGASVLT	2.6	4.8
	23	CASSEGAGGLNQPQY	1.5	4.8
	14	CASSQDGGRINEKLF	1.4	4.8
	12.2	CASSLGTGVSGASVLT	2.6	4.8
	23	CASSQTVVDAYEQY	2.7	3.6
	2.3	CASTNRDSFSQNTQY	2.4	2.4
	6.3	CASGQGVRNTEAF	1.1	2.4
	23	CASSHPGRYYEQY	2.7	2.4
	13	CASSPGTGPYSGASVLT	2.6	2.4
	13	CASSLGGYSNQPQY	1.5	2.4
	6.1	CASSEALRGIDDYT	1.2	2.4
	23	CVSSPGQLSNQPQY	1.5	1.2
	3.4	CASSQGFLRIAQLF	2.2	1.2
	23	CASSSGQLSNQPQY	1.5	1.2
	7.6	CASSSQDSNNQPQY	1.5	1.2
	23	CASSPGQLSNQPQY	1.5	1.2
	7.4	CASSLDRANTARLF	2.2	1.2
	6.2	CASSLQGNSNQPQY	1.5	1.2

C

Spearman's Rank Correlation; 0.6283
$P=0.0440$

Spearman's Rank Correlation; 0.7563
$P=0.0098$

D

Spearman's Rank Correlation; 0.2369
$P=0.4854$

Spearman's Rank Correlation; 0.07853
$P=0.8179$
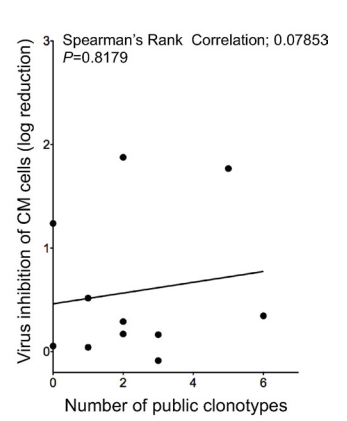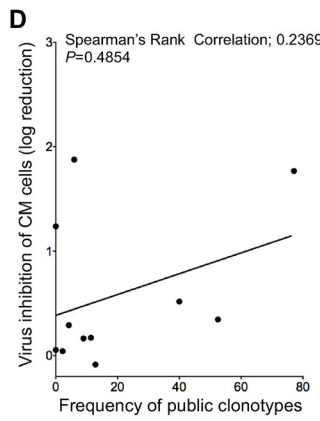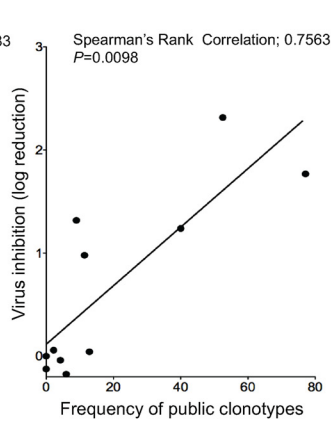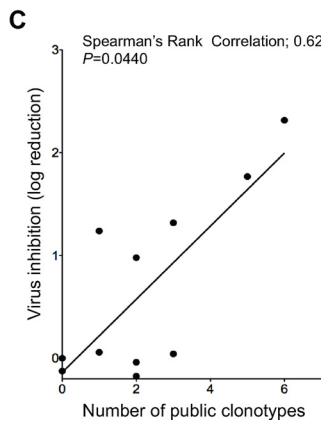
CD8$^+$ T cells (FASLG, 4-1BB, and HVEML) in stimulated cells compared to that in nonstimulated cells.

We then compared the gene profiles of CM9-stimulated EM CD8$^+$ T cells from monkeys with strong VIA and those from monkeys with weak VIA ($n = 3$ and 2, respectively). Stimulated CM9-specific EM CD8$^+$ T cells from monkeys with strong VIA were transcriptionally distinct from those from monkeys with weak VIA (Fig. 2C; see also Table S2 in the supplemental material). Single-gene analysis (Fig. 2D) revealed the increased expression of cytokines (TNF and IL-2), chemokines (CCL5 and CCL3L1), a transcription/activation marker (CD69), and cytolytic molecules related to the killing activity of CD8$^+$ T cells (FASLG, PRF1, GrzA, GrzK, 4-1BB, and HVEML) in monkeys with strong VIA compared to that in monkeys with weak VIA. Of note, the increased expression of PRF1, GrzA, and GrzK was apparent only in the comparison between strong and weak VIAs, indicating that the amount of endogenous expression of these genes was higher for strong than for weak VIA. We also identified several canonical pathways that were differentially regulated in peptide-stimulated CM9-specific EM CD8$^+$ T cells when comparing monkeys with strong VIA and those with weak VIA (see Fig. S3A in the supplemental material). Furthermore, biological functions related to protein synthesis, RNA posttranscriptional modification, gene expression, cell death, and cellular development were also profoundly different (see Fig. S3B in the supplemental material). The canonical pathway of apoptosis signaling was also found to be significant (see Fig. S3C in the supplemental material). Caspase8/10 and caspase2 were decreased and Bfl-1 was upregulated in association with strong VIA compared to levels with weak VIA. These data suggest an enhanced antiapoptotic status of CM9-specific EM CD8$^+$ T cells for strong VIA compared to that for weak VIA.

Functional profiles of Gag CM9-specific EM CD8$^+$ T cells. We next assessed the functions of vaccine-induced CM9-specific EM CD8$^+$ T cells by polychromatic flow cytometry. Macaques with strong VIA mobilized higher levels of CD107a than macaques with weak VIA, although this comparison was not statistically significant (Fig. 3A) ($P = 0.0823$). This difference was mostly due to an increase in single-positive CD107a$^+$ cells in macaques with strong VIA, although a slight increase in the fraction of multifunctional cells was observed as well (Fig. 3B). No differences were observed with respect to the production of IL-2, IFN-γ, MIP-1β, or TNF between these two groups.

Perforin expression in CM9-specific EM CD8$^+$ T cells trended toward higher levels in the strong VIA group ($P = 0.0823$). The strong and weak VIA groups exhibited similar levels of granzyme A and granzyme B expression (Fig. 3 C). There were no significant differences in the simultaneous expression of killing molecules between the strong and weak VIA groups (Fig. 3D), although the increase in perforin staining resulted in an increase in the fractions of both multifunctional and single perforin-positive cells in the strong group. The VIA of EM CD8$^+$ T cells was positively

associated with both CD107a mobilization and perforin expression in EM CD8$^+$ T cells (CD107a, $P = 0.0074$, $r = 0.7727$; perforin, $P = 0.0336$, $r = 0.6545$) (Fig. 3E).

Public clonotype usage in Gag CM9-specific EM CD8 T cell populations predicts VIA. Next we sorted the CM9-specific CD8$^+$ T cell populations and sequenced the constituent TCRB chains (25). More CM9-specific public clonotypes were observed in macaques with strong VIA than in monkeys with weak VIA (Fig. 4A). Macaques with weak VIA possessed fewer, if any, public clonotypes within CM9-specific CD8$^+$ T cells (Fig. 4B). Although the mechanism for this predictive association is largely unknown, it has been suggested that certain public clonotypes suppress viral replication more effectively (16). Accordingly, we measured the number and frequency of public clonotypes in each SIV-infected macaque and compared these parameters with the VIA. Significant positive correlations were detected between the *in vitro* log reduction of SIV and both the number and frequency of public clonotypes within the CM9-specific EM CD8$^+$ T cell compartment (Fig. 4C). No such relationship was found in the CM CD8$^+$ T cell compartment (Fig. 4D).

DISCUSSION

Here we show that vaccine-induced VIA in EM CD8$^+$ T cells predicts better viral control in monkeys that are not protected against infection with SIVsmE660. This VIA is associated with increased expression of genes regulating cytokine, chemokine, and cytolytic molecules, functional evidence of greater degranulation, and more perforin production within the EM CD8$^+$ T cell response. Earlier work has also shown that HIV-specific CD8$^+$ T cells from elite controllers have higher perforin content and CD107a mobilization than chronically infected progressors (7, 13, 14). Even within the Mamu-A*01$^+$ macaques, we observed that these two factors correlated with the VIA of EM CD8$^+$ T cells. On this basis, we propose that it is relevant and direct to assess the function of EM CD8$^+$ T cells by VIA when evaluating HIV/AIDS vaccines.

Effector memory SIV-specific CD8$^+$ T cells targeting epitopes other than Gag CM9 contribute to the overall T cell response to SIV, and it is unclear whether our results, both in terms of VIA and public clonotypes, extend beyond this single epitope. However, our data do extend prior findings by demonstrating that public clonotype usage within protective Gag CM9-specific EM CD8$^+$ T cells is associated with *in vitro* virus inhibition. Previous work has shown that CM9-specific public clonotype usage during acute infection or after vaccination predicts the set-point VL that emerges during early-chronic-phase infection (22). However, the mechanism underlying this observation remains enigmatic. In broad terms, it has been postulated that two nonmutually exclusive effects may be at play. First, CM9-specific public clonotypes might be mobilized with more-rapid kinetics as a function of higher precursor frequencies in the naïve pool generated by the process of convergent recombination (26, 32, 33), with attendant mitigation of the mucosal immune damage that occurs during the acute

FIG 4 Clonotypic architecture of Gag CM9-specific CD8$^+$ T cells. (A and B) TRBV and TRBJ usage, CDR3β amino acid sequences, and the relative frequencies of CD8$^+$ T cell clonotypes specific for the CM9 epitope are shown for 5 macaques with strong VIA (A) and 6 macaques with weak VIA (B) at week 12 after the rAd5 boost. Colored boxes indicate public clonotypes. Public clonotypes were defined on the basis of TRB amino acid sequences that were present in more than one macaque, with reference to the present data and previously published sequences (15, 22, 23). (C) Simple linear regressions predicting the VIA of EM CD8$^+$ T cells from week 12 after the rAd5 boost by the number of public clonotypes (left) and the frequency of public clonotypes (right) present in the CM9-specific CD8$^+$ T cell population ($n = 11$). (D) Simple linear regressions predicting the VIA of CM CD8$^+$ T cells from week 12 after the rAd5 boost by the frequency of public clonotypes (left) and the number of public clonotypes (right) present in the CM9-specific CD8$^+$ T cell population ($n = 11$).

phase of infection leading to improved outcomes (4). Second, intrinsic properties of public clonotypes *per se* might explain the observed biological effects (3, 16). Indeed, it seems that public clonotypes, at least in the setting of CM9-specific CD8$^+$ T cell populations, are more cross-reactive and, hence, better able to recognize viral variants (22). Nevertheless, it remains unclear whether this is a determinative effect or an epiphenomenon. Here, we show that CM9-specific public clonotypes confer enhanced VIA within the EM CD8$^+$ T cell compartment, a parameter that was not directly assessed in previous studies. Thus, these data define a potential mechanistic basis for the observed protective effects of public clonotypes in this setting and emphasize the potential importance of TCR repertoire analyses as a component of immune monitoring in HIV/SIV vaccine trials (1).

It has been reported that antigen-specific EM CD8$^+$ T cells elicited by vaccination with rhesus cytomegalovirus (RhCMV) vectors can profoundly control SIV after intrarectal SIV challenge in some macaques (11, 12). Using these vectors, high frequencies of SIV-specific EM CD8$^+$ T cells are elicited at potential sites of virus replication in rhesus macaques that stringently control highly pathogenic SIVmac239 infection early after mucosal challenge. Our results support the role of EM CD8$^+$ T cells in the control of HIV/SIV infection, although antigen-specific CD8$^+$ T cells elicited by DNA-rAd5 vaccination were unable to exert the profound control observed after RhCMV/SIV vaccination. The plasmid DNA prime-rAd5 boost vaccine used in this study was strongly immunogenic (11) and induced both CD8$^+$ T cell responses and Env-specific antibody responses. Indeed, both neutralizing antibodies (which were associated with protection against acquisition) and EM CD8$^+$ T cells with strong VIA (which were associated with virologic control after infection) were induced. This vaccine approach offers the potential to decrease the incidence of HIV acquisition after sexual exposure and enhance immune control of viral replication even after vaccine breakthrough infection.

ACKNOWLEDGMENTS

REFERENCES

1. **Appay V, Douek DC, Price DA.** 2008. CD8+ T cell efficacy in vaccination and disease. Nat. Med. **14**:623–628.
2. **Argaet VP, et al.** 1994. Dominant selection of an invariant T cell antigen receptor in response to persistent infection by Epstein-Barr virus. J. Exp. Med. **180**:2335–2340.
3. **Berger CT, et al.** 2011. High-functional-avidity cytotoxic T lymphocyte responses to HLA-B-restricted Gag-derived epitopes associated with relative HIV control. J. Virol. **85**:9334–9345.
4. **Brenchley JM, Price DA, Douek DC.** 2006. HIV disease: fallout from a mucosal catastrophe? Nat. Immunol. **7**:235–239.
5. **Cohen MS, Shaw GM, McMichael AJ, Haynes BF.** 2011. Acute HIV-1 Infection. N. Engl. J. Med. **364**:1943–1954.
6. **Douek DC, et al.** 2002. A novel approach to the analysis of specificity, clonality, and frequency of HIV-specific T cell responses reveals a potential mechanism for control of viral escape. J. Immunol. **168**:3099–3104.
7. **Freel SA, et al.** 2010. Phenotypic and functional profile of HIV-inhibitory CD8 T cells elicited by natural infection and heterologous prime/boost vaccination. J. Virol. **84**:4998–5006.
8. **Gaucher D, et al.** 2008. Yellow fever vaccine induces integrated multilineage and polyfunctional immune responses. J. Exp. Med. **205**:3119–3131.
9. **Gentleman RC, et al.** 2004. Bioconductor: open software development for computational biology and bioinformatics. Genome Biol. **5**:R80.
10. **Goonetilleke N, et al.** 2009. The first T cell response to transmitted/ founder virus contributes to the control of acute viremia in HIV-1 infection. J. Exp. Med. **206**:1253–1272.
11. **Hansen SG, et al.** 2011. Profound early control of highly pathogenic SIV by an effector memory T-cell vaccine. Nature **473**:523–527.
12. **Hansen SG, et al.** 2009. Effector memory T cell responses are associated with protection of rhesus monkeys from mucosal simian immunodeficiency virus challenge. Nat. Med. **15**:293–299.
13. **Hersperger AR, et al.** 2011. Increased HIV-specific CD8+ T-cell cytotoxic potential in HIV elite controllers is associated with T-bet expression. Blood **117**:3799–3808.
14. **Hersperger AR, et al.** 2010. Perforin expression directly ex vivo by HIV-specific CD8 T-cells is a correlate of HIV elite control. PLoS Pathog. **6**:e1000917.
15. **Hryniewicz A, et al.** 2007. Interleukin-15 but not interleukin-7 abrogates vaccine-induced decrease in virus level in simian immunodeficiency virus mac251-infected macaques. J. Immunol. **178**:3492–3504.
16. **Iglesias MC, et al.** 2011. Escape from highly effective public CD8+ T-cell clonotypes by HIV. Blood **118**:2138–2149.
17. **Koup RA, et al.** 1994. Temporal association of cellular immune responses with the initial control of viremia in primary human immunodeficiency virus type 1 syndrome. J. Virol. **68**:4650–4655.
18. **Lamoreaux L, Roederer M, Koup R.** 2006. Intracellular cytokine optimization and standard operating procedure. Nat. Protoc. **1**:1507–1516.
19. **Letvin NL, et al.** 2011. Immune and genetic correlates of vaccine protection against mucosal infection by SIV in monkeys. Sci. Transl. Med. 3:81ra36.
20. **National Research Council.** 1996. Guide for the care and use of laboratory animals. National Academy Press, Washington, DC.
21. **Pantaleo G, et al.** 1994. Major expansion of CD8+ T cells with a predominant V beta usage during the primary immune response to HIV. Nature **370**:463–467.
22. **Price DA, et al.** 2009. Public clonotype usage identifies protective Gag-specific CD8+ T cell responses in SIV infection. J. Exp. Med. **206**:923–936.
23. **Price DA, et al.** 2004. T cell receptor recognition motifs govern immune escape patterns in acute SIV infection. Immunity **21**:793–803.
24. **Quakkelaar ED, et al.** 2011. Improved innate and adaptive immunostimulation by genetically modified HIV-1 protein expressing NYVAC vectors. PLoS One **6**:e16819.
25. **Quigley MF, Almeida JR, Price DA, Douek DC.** 2011. Unbiased molecular analysis of T cell receptor expression using template-switch anchored RT-PCR. Curr. Protoc. Immunol. **10**:Unit10.33.
26. **Quigley MF, et al.** 2010. Convergent recombination shapes the clonotypic landscape of the naive T-cell repertoire. Proc. Natl. Acad. Sci. U. S. A. **107**:19414–19419.
27. **R Development Core Team.** 2010. R: a language and environment for statistical computing. R Foundation for Statistical Computing, Vienna, Austria. www.R-project.org.
28. **Schmitz JE, et al.** 1999. Control of viremia in simian immunodeficiency virus infection by CD8+ lymphocytes. Science **283**:857–860.
29. **Smyth GK.** 2004. Linear models and empirical Bayes methods for assessing differential expression in microarray experiments. Stat. Appl. Genet. Mol. Biol. **3**:Article3.
30. **Turner SJ, Doherty PC, McCluskey J, Rossjohn J.** 2006. Structural determinants of T-cell receptor bias in immunity. Nat. Rev. Immunol. **6**:883–894.
31. **Venturi V, et al.** 2006. Sharing of T cell receptors in antigen-specific responses is driven by convergent recombination. Proc. Natl. Acad. Sci. U. S. A. **103**:18691–18696.
32. **Venturi V, Price DA, Douek DC, Davenport MP.** 2008. The molecular basis for public T-cell responses? Nat. Rev. Immunol. **8**:231–238.
33. **Venturi V, et al.** 2011. A mechanism for TCR sharing between T cell subsets and individuals revealed by pyrosequencing. J. Immunol. **186**:4285–4294.